Planning the Trajectories of Multiple Mobile Sinks in Large-Scale, Time-Sensitive WSNs

Wint Yi Poe, Michael Beck, Jens B. Schmitt

Distributed Computer Systems Lab (DISCO), University of Kaiserslautern, Germany

***Abstract*—Controlled sink mobility has been shown to be very beneficial in lifetime prolongation of wireless sensor networks (WSNs) by avoiding the typical hot-spot problem near the sink. Besides striving for elongated lifetimes, many applications of WSNs are time-sensitive, i.e., they strongly benefit from bounds on the message transfer delay. Further, large WSNs require *multiple* sinks in order to scale well with respect to delay and lifetime. Therefore, it becomes very interesting to investigate how to plan the trajectories of multiple mobile sinks such that lifetime and delay goals are met simultaneously. To that end, we propose a geometrically principled heuristic for finding good trajectories of multiple mobile sinks in large-scale, time-sensitive WSNs. First, we discuss the high analytical challenges of optimally planning the trajectories of multiple mobile sinks. Based on this, we relax the problem by transforming it into a geometric design problem, which, subsequently, is solved in closed form. In simulations, we investigate how well this geometric heuristic for sink trajectories of multiple mobile sinks performs with respect to delay and lifetime. We find that it excels especially in large-scale WSNs, for example in a WSN with 500 nodes and 20 sinks, it roughly cuts delay bounds by 50% while tripling the lifetime compared to the sinks following random walks. Hence planning the sink trajectories carefully really pays off.**

I. Introduction

Mobility is a mixed blessing for wireless sensor networks (WSNs). On the one hand, the degree of network dynamics induced by mobile nodes or sinks may aggravate the design of networking protocols and distributed algorithms. On the other hand, *controlled mobility* also creates opportunities [5]. One of the successful ways to apply controlled mobility in WSNs is to use a mobile sink in order to avoid the typical hot-spot problem around a static sink [6], [2]. By moving the sink throughout the sensor field, the burden of being a direct neighbor of the sink can be shared among all nodes of the network and the network lifetime increases.

In general, sink mobility as, for example, using random walks of multiple mobile sinks, increases the maximum information transfer delay over that of a proper placement of a set of stationary sinks. This is simply due to the fact that there is always a delay-optimal placement of the sinks and if the sinks move away from it the message transfer delay becomes worse. Clearly, this creates a problem for time-sensitive WSN applications. So, using sink mobility, we face a conflict between lifetime maximization and delay bound minimization in large-scale, time sensitive WSNs. The challenge thus becomes to find good trajectories for the sinks such that lifetime and delay goals are met simultaneously. In this paper, we first provide a multi-objective optimization problem formulation for planning the trajectories of multiple mobile sinks, called OST (Optimal Sink Trajectory). We remark that already the single objective problem of maximizing network lifetime is known to be NP-hard [6]. Hence, we relax the OST problem by giving it a geometric interpretation, called GST (Geometric Sink Trajectory). The intuition behind this is that both, delay and lifetime, benefit from nodes being closer in terms of Euclidean distance to their assigned sinks. So, the two objectives are amalgamated into one. Furthermore, the GST lends itself to a solution based on the kernel insight that, for a single sink, the problem is reduced to simply finding a minimum enclosing circle, whose center is the optimal position for the sink to minimize the maximum Euclidean distance. Extending this insight we propose a geometrically principled approach using a polar grid to divide the sensor field into areas of similar size, each of which is the responsibility of a single sink. The sinks are moved synchronously (e.g., once a day) along an inner and an outer orbit. The optimal size of the inner and outer orbit as well as the optimal number of sinks on inner and outer orbit are derived in closed form using geometric arguments.

The rest of the paper is organized as follows. Section II provides an overview of related work. Section III describes the network model and, in order to reveal the structure of the problem, provides the original problem formulation for the OST. Next, the GST and its derivations are presented in Section IV. The performance of the polar grid-based trajectory for multiple sinks is evaluated and compared against several alternatives using simulations in Section V. We conclude the paper in Section VI.

II. Related Work

In literature, a number of works rise to the challenge of using multiple mobile sinks [4], [3], yet often not delving into the optimal planning of their trajectories. Sink trajectories can be categorized into random, state-dependent, and predefined. Usage of a random trajectory can, e.g., be found in [3] where mobile sinks perform a random walk and collect the data from the sensors of their assigned clusters trying to achieve a load balancing and lifetime maximization. Recently, [2], [14] address state-dependent sink mobility for maximizing the lifetime of WSNs. In their approach, the sink trajectory is a function of a particular network variable, such as, e.g., the state of nodes' batteries; the sink moves either grid-based [2] or following a straight line [14]. Though the lifetime performance of such trajectories is good, the methods assume knowledge of global and dynamic information for determining the optimal paths and sojourn times, which is a very strong assumption in large-scale WSNs. [4], [13] propose a predefined single sink trajectory independent of any network state such that the sink appears on the same path periodically. Interestingly,

[13] considers a predefined trajectory along concentric circles separated by $2r_{tx}$, where r_{tx} is the transmission range of node, with the aim of minimizing the total energy consumption. This is very related to our polar grid-based trajectory, yet ours is designed for multiple mobile sinks and takes lifetime as well as delay goals into account. In contrast to a periodical movement, the work in [6] proposes a predefined sink trajectory where the sink only appears once at each position along the trajectory. The author studied the improvement of lifetime prolongation by using a joint sink mobility and routing scheme similar to [7]. Most of these studies are concerned with the lifetime prolongation of a WSN, often restricting to the single sink case.

In our work, we tackle the problem of finding good trajectories for multiple mobile sinks such that we keep the maximum message delay low and still achieve a long lifetime. So, delay and energy are traded off against each other. Along similar lines, [14] optimizes this trade-off, too, designing a trajectory for a "data mule" which collects the data from each sensor node directly [10]. Yet, the data mule approach incurs long latencies and is generally not applicable in time-sensitive WSNs.

In [15], [7], [6], the movement of a sink is abstracted as a sequence of a static sink placements assuming that the time scale of sink mobility is much larger than that of data delivery; we follow this assumption in our work. Methodologically similar to our work in using geometric arguments, [6] focuses on minimizing the *average* distance between sink and assigned sensor nodes. The reasonable assumption is that in a multi-hop network, the energy cost of transmitting a message from the node to the sink is linearly proportional to the Euclidean distance between them. Such a distance-related assumption is also at the heart of our work but with additional consideration of a message transfer delay bound, which is why we set out to minimize the *maximum* distance.

III. Network Model and Problem Statement

In this section, we first provide our network model along with some basic assumptions and, next, state the problem of planning sink trajectories for multiple mobile sinks as a multi-objective optimization problem. Here, the intention is to shed light on its basic mathematical structure without providing a solution approach yet.

A. Network Model

V is the set of sensor nodes with $|V| = N$; S is the set of sinks with $|S| = K$. We model the WSN as a directed graph, $G = (\mathcal{V}, \mathcal{E})$, where $\mathcal{V} = V \cup S$. For all $a, b \in \mathcal{V}$, $\exists (a, b) \in \mathcal{E}$ if and only if a and b are within a disc-based transmission range r_{tx}.

- We assume that the sinks' movement is synchronous, i.e., all sinks move at the same time. Further, sink movement takes places on relatively long time-scales (e.g., once a day), much larger than the time-scale of the message transfer delay from sensors to sinks (e.g., on the order of seconds). Therefore, we neglect the time periods when the sinks are actually moving (or being moved) and the sink mobility is abstracted as a sequence of sinks' locations. At each location the sinks stay for an equal amount of time, further on called epoch $n = 0, 1, 2, \ldots$ In particular, we also assume that all data is flushed from the WSN before a sink movement takes place, i.e., there is no data dependency between epochs.
- The sensor nodes are assumed to be homogeneous and uniformly distributed: They send $L(n)$ data packets in each epoch n and have the same initial energy budget E available. We focus on the energy consumption for transmitting and receiving data, since the energy consumption by other units of sensor node is relatively the same for all nodes and, as such, can be taken as a constant. Also, the sensor nodes are stationary.
- We define the locations of sink s in epoch n as $l_s(n) \in \mathbb{R}^2$, and by $l(n) \in \mathbb{R}^{2\times K}$ we denote the sinks' placement in epoch n.
- For node to sink assignment, we define $x_{v,s}(n)$ as a binary variable which is set to 1 if node v is allocated to sink s in epoch n and 0 otherwise. Hence, the overall assignment $X(n)$ in epoch n is a binary matrix:
$$X(n) := (x_{v,s}(n))_{v\in V, s\in S} \in \{0,1\}^{N\times K}.$$
- For a certain assignment $X(n)$ we can define a routing as follows:
$$P_{X(n)} := \bigcup_{v\in V, s\in S\,:\, x_{v,s}(n)=1} P_{v,s}$$
where, $P_{v,s}$ is a path from node v to sink s which is described as the set of edges lying on this path under the assumption of multi-hop communication.
- We call a sequence of triples
$$\big(l(n), X(n), P_{X(n)}\big)_{n\in\mathbb{N}} =: \mathcal{S}_n$$
a strategy.
- We define the network lifetime by the timespan until the first node dies due to battery depletion.

B. Optimal Sink Trajectory: Problem Statement

Based on these definitions, we formulate the optimization problem of finding sink trajectories for multiple sinks in a WSN with the aim of minimizing the maximum delay and maximizing the network lifetime T of the network:

$$\min_{\mathcal{S}_n} \max_{v\in V,\, n\in\mathbb{N}} D_v(n)$$
$$\max_{\mathcal{S}_n} T$$

subject to: $\forall n \in \mathbb{N}$

$$\sum_{e\in\delta^-(v)} f_n(e) - \sum_{e\in\delta^+(v)} f_n(e) = L \quad \forall v \in V \tag{1}$$

$$\sum_{e\in\delta^+(s)} f_n(e) = L(n) \sum_{v\in V} x_{v,s}(n) \quad \forall s \in S \tag{2}$$

$$\sum_{s\in S} x_{v,s}(n) = 1 \quad \forall v \in V \tag{3}$$

$$\sum_{n=0}^{T} \left(\sum_{e\in\delta^-(v)} E_{tx}(e, f_n(e)) + \sum_{e\in\delta^+(v)} E_{rcv}(e, f_n(e)) \right) \le E \quad \forall v \in V \tag{4}$$

where $\delta^-(v) = \{e \in \mathcal{E} | e = (v, n), n \in \mathcal{V}\}$ and $\delta^+(v) = \{e \in \mathcal{E} | e = (n, v), n \in \mathcal{V}\}$. The function $f_n : \mathcal{E} \to \mathbb{R}^+$ describes

the amount of data sent over an edge in epoch n. Equations (1) and (2) are flow balance equations to ensure that no additional data is produced or any data is lost at the nodes. Equation (3) enforces that a sensor node is assigned to exactly one sink in epoch n. The energy constraint for each node $v \in V$ is defined in Equation (4); here, the total energy consumption for reception $E_{rcv}(e, f_n(e))$ and transmission $E_{tx}(e, f_n(e))$ up to epoch T, the lifetime of the WSN, must not exceed the initial energy E for any nodes.

The delay function $D_v(n)$ represents the end-to-end delay characteristics for the message transfer from node v to its assigned sink in epoch n. At this point, we still remain abstract about whether, e.g., an average delay over an epoch or the maximum delay experienced is taken. However, later on (in the simulations as presented in Subsection V-D), based on sensor network calculus [9], we use a bound on the maximum end-to-end delay to instantiate $D_v(n)$. In any case, the delay function $D_v(n)$ is a very complex function, which does not only depend on the path from the node v to its sink, but also on all other paths interfering with it. Hence, differences in choosing a path for just one node-sink pair, in general, affect multiple end-to-end delays. Similarly, we also remain abstract about the energy functions E_{rcv} and E_{tx}, which are also complex functions, thus aggravating the problem further. A last but not least hardness of the problem stems from the two objective functions and their conflicting nature.

IV. Geometric Sink Trajectory (GST)

Due to its fundamental hardness, we relax the OST problem, which is basically a graph problem, into a geometric one, called the Geometric Sink Trajectory (GST) problem. Basing on the assumption of a large-scale WSN with a more or less uniform node distribution we abstract from nodes as such. For the geometric shape of the sensor field we assume it to be a circle, a somewhat arguable, but often made assumption on this level of abstraction [6]. We briefly come back to a discussion about the circular shape in Section VI.

Under these abstractions for the GST, the objective of minimizing the maximum delay is reduced to the objective of minimizing the maximum Euclidean distance $d_{v,s}(n) = \|l_s(n) - pos(v)\|_2$ from sink $s \in S$ to node $v \in V$ in epoch n; here, $pos(v)$ refers to the position of sensor node v in the Euclidean space. Somewhat more indirectly, we cater for the lifetime maximization by partitioning the sensor field into areas of similar size (per epoch), each of which is under the responsibility of a single sink. The rationale of this being that each sink is roughly assigned a similar number of sensors thus leading towards a good balancing of the forwarding load between areas.

Interestingly, for the single sink case, we remark that by simply substituting the delay function by the Euclidean distance, and neglecting the energy issues, the OST problem becomes a well-known minimum enclosing circle problem [11] (we point out, though, that with K circles the problem remains hard). This problem and its solution by a minimum enclosing circle is illustrated in Figure 1. The center of such a circle is the optimal placement for a sink in terms of minimizing the maximum distance between sink and sensor nodes. We recur to this basic insight several times further on, when we look for optimal positions of sinks in their respective area.

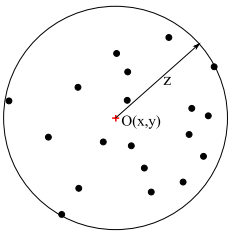

Fig. 1. An example of a minimum enclosing circle.

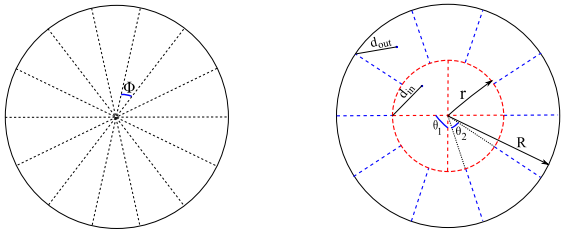

Fig. 2. Sinks assignment in (a) an equal sectorization, and (b) a polar grid.

Our framework to construct sink trajectories $l(n)$ based on solutions to the GST consists of the following steps:

1) We assign areas of similar sizes to the sinks (→lifetime maximization). In fact, there are different possibilities to achieve this and we discuss them in the following subsection.
2) After that we calculate the optimal placement of the sinks, such that the maximal distance of any point in these areas to its sink is minimized (→delay minimization).
3) Finally we define the sink trajectory for each sink by specifying its movement to the next position.

A. The Area Assignment Problem

The area assignment problem is: How to partition a circular network of radius R in order to achieve areas of similar size with respect to a given number of sinks K? A first and exact solution is an equal sectorization which has a nice scalability property in terms of handling an increasing number of sinks K without compromising the equal size of each sector. No matter how large K is, equal sectorization achieves equally sized areas by calculating the center angle of each sector as $\Phi = \frac{2\pi}{K}$. Figure 2(a) shows an example of equal sectorization for a 14 sinks network. Due to its symmetrical nature, it is sufficient to find a minimum enclosing circle for one of the circular sectors. Although, the equal sectorization achieves beneficial properties like scalability, congruity, and simplicity, the area of each circular sector becomes increasingly narrower for a growing number of sinks K, which results in relatively large maximum distances to a sink. In fact, the maximum distance for a point to its sink in a circular sector is bounded from below by $\frac{R}{2}$. This implies that the delay performance does not improve significantly any more after a certain number of sinks is reached even if more sinks are available.

Therefore, we introduce an alternative way of partitioning the sensor field, which is designed to improve on minimizing the maximum distance for a growing number of sinks K. The idea is to have two concentric circles of radii r and R, as illustrated in Figure 2(b). By dividing the circle into two

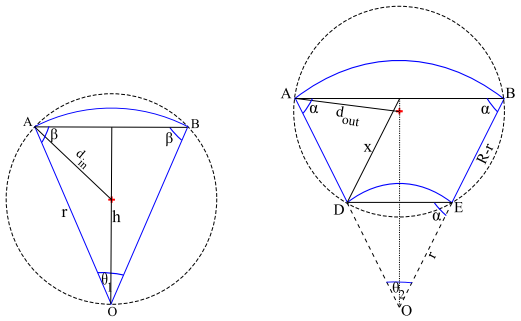

(a) (b)

Fig. 3. Circumscribed circles of polar grid cells: (a) a sector in the inner circle, and (b) an annular segment in the annulus.

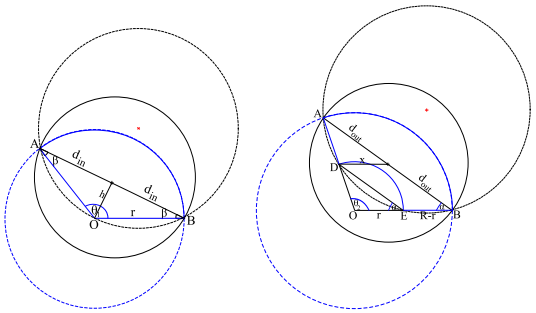

(a) Sector Segment (b) Annular Segment

Fig. 4. Optimal sink placement inside a sector and an annular segment with large $\frac{|AB|}{2}$.

different parts, the maximum distance between any point to its sink can be reduced effectively and the resulting scheme still can achieve a balanced area assignment. The resulting partition is usually called a polar grid. The following section describes how to find the optimal sink distribution in a polar grid, i.e., how many of the sinks to place in the outer ring together with the optimal value for the radius of the inner circle r.

B. Optimization of the Polar Grid Area Assignment

As shown in Figure 2(b), sinks are assigned in the inner circle and in the annulus of the outer circle to create a polar grid. We define K_{in} and K_{out} as the number of sinks for the inner circle and the annulus, respectively. Figure 2(b) illustrates an example of 14 sinks with $K_{in} = 4$ and $K_{out} = 10$. Let us define d_{in} and d_{out} as the minimal radii of enclosing circles for the sector and annular segment, respectively, given r, K_{in} and K_{out}. Then, the polar grid-based area assignment problem can be formulated as:

$$\min_{0<K_{in}\leq K} \min_{0\leq r\leq R} \max\left\{d_{in}, d_{out}\right\}. \tag{5}$$

We calculate d_{in} and d_{out} from the corresponding minimum enclosing circles. In the following we assume K_{in}, $K_{out} \geq 3$ to avoid degenerate cases.

1) Formulation of d_{in} and d_{out}: There are two types of cells in the polar grid-based assignment scheme: a sector in the inner circle and an annular segment in the annulus of the outer circle. The optimal values of K_{in} and K_{out} are likely to be unequal in general, which implies two different center angles θ_1 and θ_2 for sector and annular segment, respectively. This is also illustrated in Figure 3(a) and (b).

We find the minimum enclosing circle and its radius by approximating each polar grid cell by an easier shape. In particular, we determine the minimum enclosing circles for the isosceles triangle and isosceles trapezoid for the respective polar grid cells. In Figure 3(a) and (b), the minimum enclosing circles for the isosceles triangle $\triangle ABO$ and the isosceles trapezoid $ABDE$ are depicted, which, in this case, are the circumscribing circles of the triangle and trapezoid, respectively.

d_{in} and d_{out} are calculated from the respective minimum enclosing circles formulation. Given r, R, α and β (see Figure 3 and 4), the following equations characterize d_{in} and d_{out}:

$$d_{in} = \begin{cases} \frac{r}{2\sin\beta} & \text{for } \frac{|AB|}{2} \leq h \\ r\cos\beta & \text{for } \frac{|AB|}{2} \geq h \end{cases} \tag{6}$$

$$d_{out} = \begin{cases} \frac{\sqrt{(R-r)^2+4rR\cos^2\alpha}}{2\sin\alpha} & \text{for } \frac{|AB|}{2} \leq x \\ R\cos\alpha & \text{for } \frac{|AB|}{2} \geq x \end{cases} \tag{7}$$

Note that $\frac{|AB|}{2} \leq x$ is equivalent to $r \leq R - 2R\cos^2\alpha$ and $\frac{|AB|}{2} \leq h$ is equivalent to $0 \leq \theta_1 \leq \frac{\pi}{2}$. It can be shown that the approximations of using a triangle and a trapezoid for sector and annular segment, respectively, actually deliver the same results with respect to the optimal sink placement as the original shapes. Due to space restrictions, we omit the mathematical proof of this statement and refer the interested reader to [8].

2) Optimal r and sink distribution K_{in} vs. K_{out}: Based on the mathematical formulations for d_{in} and d_{out}, we are able to evaluate expression (5). As one can see in the previous subsection d_{in} is strictly increasing in r and d_{out} is non-increasing in r for any fixed K_{in} and K_{out}. Hence there exists a unique intersection between these two functions. This intersection is the minimum of $\max\{d_{in}, d_{out}\}$ as a function of r.

In the first case of Equation (6) the necessary calculations to find the minimum of $\max\{d_{in}, d_{out}\}$ are:

$$\begin{aligned} \frac{r}{2\sin\beta} &= \frac{\sqrt{(R-r)^2+4rR\cos^2\alpha}}{2\sin\alpha} \\ \Rightarrow \quad r_1, r_2 &= \frac{-b \pm \sqrt{b^2-4ac}}{2a} \\ r_0 &= R - 2R\cos^2\alpha, \end{aligned} \tag{8}$$

where

$$\begin{aligned} a &= \sin^2\alpha - \sin^2\beta, \\ b &= 2R\sin^2\beta(1-2\cos^2\alpha), \\ c &= -R^2\sin^2\beta. \end{aligned}$$

By taking the minimum of $[r_0]_+$, r_1 and r_2 we can find the optimal radius for this case.

If we use instead the second case of Equation (6) the computations are quite similar and look like follows:

$$\begin{aligned} r_1, r_2 &= \frac{-e \pm \sqrt{e^2-4df}}{2d} \\ r_0 &= R - 2R\cos^2\alpha, \end{aligned}$$

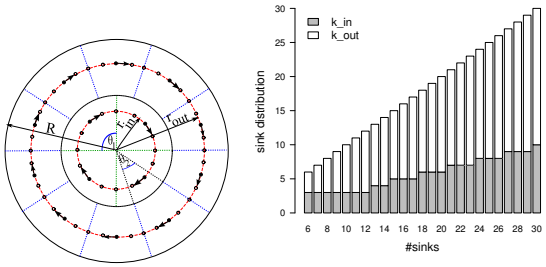

(a) (b)

Fig. 5. (a) An example of polar grid_based trajectory for a 14 sinks network, and (b) optimal sink distributions (K_{in} vs. K_{out}) for the polar grid-based area assignment.

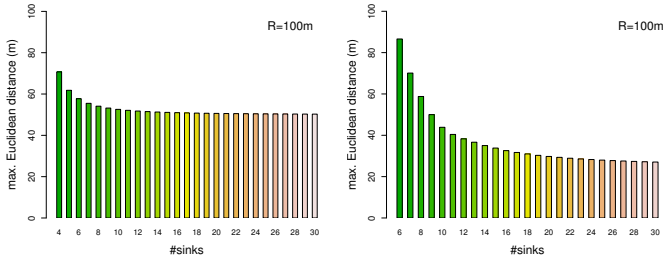

(a) (b)

Fig. 6. The maximum Euclidean distances distribution of (a) an equal sectorization, and (b) a polar grid-based area assignment schemes.

where

$$\begin{aligned} d =& 4\sin^2\alpha\cos^2\beta - 1, \\ e =& 2R - 4R\cos^2\alpha, \\ f =& -R^2. \end{aligned}$$

Again the minimum of $[r_0]_+$, r_1 and r_2 is the optimal value for r.

For a given K and R, we can now exhaustively search for the optimal values of r trying all possible combinations of K_{in} and K_{out} (the size of the search space is just $K-5$ since we assume $K_{in},\ K_{out} \geq 3$). Among all combinations, we select the best configuration of K_{in} and K_{out} with respect to the minimum distance of d_{in} and d_{out} (using the best r), thus implementing Equation (5).

C. Designing the Sinks' Trajectories

Now, we know the optimal points (i.e., the centers of the minimum enclosing circles for sector and annular segments) which produce the optimal d_{in} and d_{out}. Based on these points, we design circular mobile sink trajectories. Let r_{in} and r_{out} denote the distances from the center of the network to the center of the minimum enclosing circles for the sector and annular segment, respectively, as illustrated in Figure 5(a).

The radii r_{in} and r_{out} are defined by:

$$r_{in} = \begin{cases} \frac{r}{2\sin\beta} & \text{for } \frac{|AB|}{2} \leq h \\ r\sin\beta & \text{for } \frac{|AB|}{2} \geq h \end{cases} \tag{9}$$

and

$$r_{out} = \begin{cases} R\sin\alpha & \text{for } \frac{|AB|}{2} \leq x \\ \sqrt{\frac{(R-r)^2+4rR\cos^2\alpha}{4\sin^2\alpha} - r^2\cos^2\alpha} + r\sin\alpha & \text{for } \frac{|AB|}{2} \geq x \end{cases} \tag{10}$$

The trajectories of the sinks basically result from rotating the whole polar grid in an attempt to keep both, message transfer delay and load per sink, balanced. Clearly, an interesting parameter is how far we rotate the polar grid, i.e., which step size we use for each sink when going from one epoch to the other. Results concerning this step size and a deeper discussion of its influence are provided in Section V.

D. Analytical Evaluation of the Geometric Sink Trajectory

Before we delve into a detailed simulative study of our approach, we first analytically compare the equal sectorization and polar grid-based area assignment schemes with each other. Figure 6(a) and (b) show the maximum distance distributions of an equal sectorization- and a polar grid-based area assignment for $R = 100\,m$ and a varying number of sinks K up to 30. Apparently, a polar grid area assignment effectively reduces the maximum distance as K grows. Note that for $K \leq 8$ the equal sectorization is in fact superior to the polar grid. The reason lies in the restriction of having $K_{in},\ K_{out} \geq 3$, otherwise the polar grid should always be superior, since equal sectorization can be considered a special case of a polar grid (with $K_{out} = 0$ and $r = R$). The results are based on the optimal choice for r and the optimal sinks distribution for K_{in} and K_{out}.

We further show the corresponding optimal sink distribution K_{in} and K_{out} in Figure 5(b). Starting from $K = 13$, the value of K_{in} is $\lfloor \frac{K}{3} \rfloor$ and consequently the value of K_{out} becomes $\lceil \frac{2K}{3} \rceil$. Therefore, the optimal ratio of $\frac{K_{in}}{K_{out}}$ becomes $\frac{1}{2}$. In general, the optimal sink distribution is about one third of the sinks for the inner circle and about two-thirds for the annulus. Furthermore, we observed that the optimal r is converging to half of the radius R under the optimal sink distribution.

We remark that, in general, the polar grid does not achieve a perfectly equal area assignment. Nevertheless, the differences are not too large and as discussed in the following section the polar grid performs favorably with respect to both objectives, lifetime maximization and delay minimization.

V. Performance Evaluation

In this section, using discrete-event simulations, we evaluate the performance of the polar grid-based solution to the GST under the assumptions of the original OST problem formulation. In particular, we compare it to a number of alternative sink trajectories with respect to delay and lifetime performance. Furthermore, we analyze factors like the number of sensor nodes, the number of sinks, and the movement step sizes of the sinks.

A. Competitors

We selected three competing sink trajectories which are illustrated in Figure 7(a), (b), and (c). Supposedly as a lower bound among the trajectories, using a random walk (with a fixed step size) for each of initially randomly placed sinks is

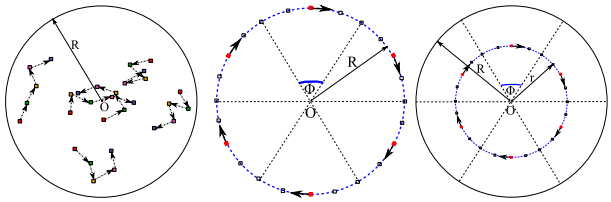

(a) (b) (c)

Fig. 7. Competitors: (a) a random walk, (b) an outer periphery, and (c) an equal sectorization trajectory.

selected. Clearly, this is a very simple strategy which shall serve as a reference in how far investing more effort in the planning of sink trajectories is justified.

The next competitor is based on an insight by Luo for the single sink case (see Claim 7 in his thesis [6]): using the outer periphery for the sink is actually optimal with respect to lifetime (under mild assumptions about the symmetry of the trajectory). We simply extend this into having multiple sinks circulating in equal distances from each other in the outer periphery of the WSN.

As a last competitor, Figure 7(c) illustrates an equal sectorization trajectory which, in fact, is constructed exactly as the inner circle of the polar grid-based trajectory mentioned in Figure 5(a).

Apart from the random walk trajectory, all other trajectories are predefined so that the sinks move along the corresponding trajectory repeatedly until the network dies.

B. Delay Performance

While an average delay analysis is certainly useful for some WSN applications, for time-sensitive WSNs being able to bound the worst-case delay is generally more important. To that end, we evaluate the delay performance of the the different sink trajectories using the framework of sensor network calculus (SNC) [9]. This requires to specify bounds on the arrival and service processes, called arrival and service curves, their actual settings are given in Subsection V-D.

C. Lifetime Performance

As has been mentioned in Subsection III-A, we define the lifetime of the WSN as the timespan until the first sensor node depletes its battery. In order to capture this event we need to keep track of the battery levels of each sensor node. To that end, we define a simple, yet fairly realistic model mimicking the energy consumption of MICAz motes [1]. We focus on the energy consumption of the transceiver unit. The formulation of the total energy consumption for all data transmissions from the nodes to their assigned sinks up to epoch n, is denoted by E^n_{total}; it is the sum of total energy consumption of all nodes:

$$E^n_{total} = \sum_{v \in V} E^n_v \tag{11}$$

where the energy consumption for a node v in epoch n, E^n_v, is given in accordance to Equation (4) as:

$$E^n_v = \sum_{e \in \delta^-(v)} E_{tx}(e, f_n(e)) + \sum_{e \in \delta^+(v)} E_{rcv}(e, f_n(e)),$$

with

$$E_{rcv}(e, f_n(e)) = E_{rcv}(f_n(e)) = P_{rcv} \times t_{rcv}(f_n(e)), \tag{12}$$

$$E_{tx}(e, f_n(e)) = P_{tx}(e) \times t_{tx}(f_n(e)). \tag{13}$$

In (12), we see that the energy consumption for receiving the data $f_n(e)$ is just the time needed to receive the data $t_{rcv}(f_n(e))$ multiplied by the power consumption P_{rcv} of the receiving unit; this is independent of the distance between the sending and receiving node. In (13), the energy consumption for sending data is again the time needed to send the data $t_{tx}(f_n(e))$ times the power consumption of the sending unit $P_{tx}(e)$, which, however, now is dependent on the distance between the communicating nodes. Taking the values from the MICAz data sheet [1], we can calculate the power consumed by the receiver electronics P_{rcv}. Basically, P_{tx} depends on the transmitted output power setting which again depends on the distance and the selected modulation scheme. Here, we relied on a model for the MICAz mote from the literature, please refer for more details to [12].

D. Results

The primary factors in our simulative experiments are: the number of nodes, the number of sinks, and the step sizes (i.e., the Euclidean distance between two consecutive stops). In all scenarios, nodes are uniformly distributed over a circular field with radius R. The respective network radii are chosen such that a node density of $\frac{1}{50\,m^2}$ is achieved. A $16\,m$ disc-based transmission range is used. Furthermore, sink assignment is done according to the minimum Euclidean distance between nodes and sinks, whereas shortest path routing is used for path selection. For all experiments, we performed 10 replications for each factor combination and present the average results from these. For the large majority of results, we obtained non-overlapping 95% confidence intervals, so we do not show these in most graphs for reasons of legibility.

For the SNC computations, the popular token-bucket arrival curve and rate-latency service curves are used. In particular, for the service curve we use a rate-latency function that corresponds to a duty cycle of $1\,\%$. For the $1\,\%$ duty cycle, it takes $5\,ms$ time on duty with a $500\,ms$ cycle length which results in a latency of $0.495\,s$[1]. The corresponding forwarding rate becomes $2500\,bps$.

For the lifetime evaluation, the nodes are set to an initial battery level of $0.1\,joule$. The packet size is assumed to be $100\,bytes$. Based on $\tau = 2$ for the free space propagation and using the relationship in [12], in all scenarios a packet transmission incurs a current consumption of $8.5\,mA$ with $-25\,dBm$ for distances up to $12.5\,m$, and $9.9\,mA$ for distances between $12.5\,m$ and $23\,m$ with $-20\,dBm$. Here, a transmission data rate of $250\,Kbps$ is used, which takes $t_{tx} = 3.2\,ms$ for a $100\,byte$ packet. A constant voltage of $3\,V$ is used to transmit and receive modes. We use a current of $19.7\,mA$ for the consumed power by the receiver electronics with a $1\,\%$ duty cycle for receiving a data packet. With these assumptions, we apply Equations (11) to (13).

[1]The values are calculated based on the TinyOS files CC2420AckLpl.h and CC2420AckLplP.nc.

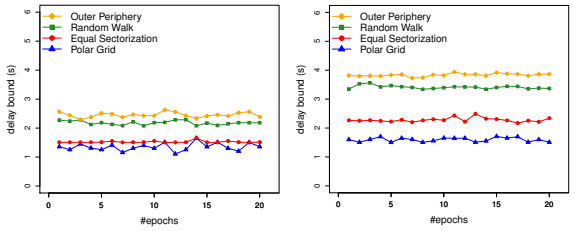

Fig. 8. The worst-case delay comparisons of (a) 200 nodes with 10 sinks network, and (b) 500 nodes with 20 sinks network.

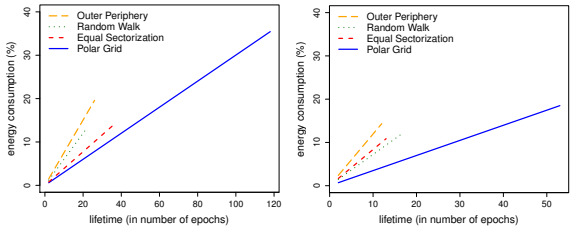

Fig. 9. The lifetime comparisons of (a) 200 nodes with 10 sinks network, and (b) 500 nodes with 20 sinks network.

1) Experiment 1: Baseline comparison: The simulation results of the worst-case delay for the different competitors over 20 epochs are shown in Figure 8(a) and (b) for a 200-nodes-10-sinks and 500-nodes-20-sinks WSN, respectively. Here, the step size of the equal sectorization trajectory resulting from a movement by a center angle of 10 degrees is used as a reference for the step sizes in the polar grid, outer periphery, and random walk trajectories.

In both scenarios, the polar grid trajectory achieves significantly lower worst-case delays than its competitors (especially in the 500 node network). On average, the polar grid achieves about $50\,\%$ lower delays than the random walk and the outer periphery and roughly $20\,\%$ lower delay than the equal sectorization. As we expected, the random walk trajectory provides a high worst-case delay. At first glance surprisingly, the outer periphery performed even worse than the random walk, though, due to the fact that the sinks are rather far away from some of the nodes this is not unreasonable. The equal sectorization produces fairly good delays in the smaller network but cannot stay close to the polar grid in the larger one. So we validated its lesser scalability in terms of delay performance as it was already indicated in the analytical evaluation in Subsection IV-D.

The results for the lifetimes of the four competitors are shown in Figure 9(a) and (b). Here, the x-axis represents the lifetime of the WSN (in number of epochs). The y-axis indicates the percentage of the total energy consumption of the whole network during the lifetime of the WSN. As can be observed, the polar grid trajectory strongly outperforms the other trajectories in both scenarios. On average, the polar grid achieves a $440\,\%$, $450\,\%$, and $330\,\%$ higher lifetime than the random walk, outer periphery, and equal sectorization trajectories, respectively. From Figure 9 it becomes clear that this is mainly for two reasons: (1) it requires less total energy per epoch and (2) it drains the energy from the sensor field in a more balanced fashion (indicated by having a higher total energy consumption when the network dies). It may be noteworthy that the equal sectorization actually performs worse than the random walk in the 500 node network indicating that it does not scale well with respect to lifetime due to a high energy consumption per epoch as well as not being successful in avoiding hot-spot problems. Similarly, the outer periphery performs worse than the random walk in the 500 node network. This is even a bit more surprising than its inferior delay performance, as single sink outer periphery trajectory maximizes lifetime. So, this indicates that the multiple sinks trajectory problem is fundamentally different from its single sink counterpart.

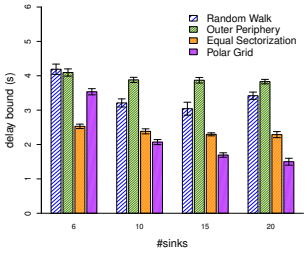

Fig. 10. Delay bound comparison under different numbers of sinks in a 500 node network.

2) Experiment 2: Varying the number of sinks: In the next experiment, the effect of the number of sinks for each of the competitors is evaluated. Apart from varying the number of sinks, we use the same settings as for Experiment 1. Figure 10 provides the results for the delay bounds under different number of sinks in a 500 node network. As can be seen, the only trajectory that is really able to exploit a growing number of sinks to reduce the delay bound significantly is the polar grid; the outer periphery and the equal sectorization are actually quite insensitive to it, the random walk exhibits a rather chaotic behavior (20 sinks are worse than 10 sinks). One may note that in the 6 sinks case the equal sectorization outperforms the polar grid. This, as already discussed in Subsection IV-D, is due to the artefact that $K_{in}, K_{out} \geq 3$ disables an effective optimization of the polar grid trajectory for this small number of sinks. In a certain sense it shows that an unoptimized polar grid can also perform unfavorably.

3) Experiment 3: Varying step sizes: From Experiment 1 and 2, we can clearly see that the polar grid trajectory is a promising heuristic for minimizing the worst-case delay and maximizing the lifetime of large-scale WSNs. In this last experiment, we now investigate the effect of varying the step size of the polar grid trajectory. For this, we focus on the lifetime performance for different step sizes as the delay performance is not particularly sensitive to it. Figure 11(a) and (b) show the lifetimes of the polar grid trajectory for different step sizes in a 200 node network with 10 sinks (here (b) provides a zoom-in for an interesting range of (a)). The interpretation of the x-axis is as follows: based on the center angle of an annular segment $\theta_2 = \frac{2\pi}{K_{out}}$, the different step sizes are computed as $\frac{\theta_2}{n}$, where n represents the value displayed on the x-axis; this means the x-axis runs from large step sizes to very small ones. More specifically, the optimal value of K_{out}

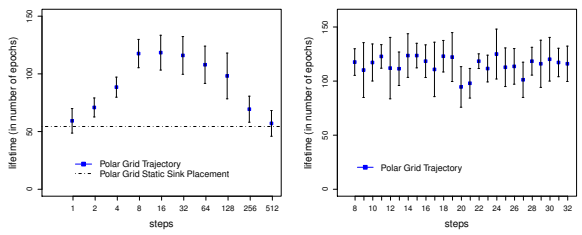

(a) (b)

Fig. 11. Lifetime comparisons under varying step sizes in a 200 nodes with 10 sinks network.

in this experiment is 7 (out of 10 sinks) and thus $\theta_2 = \frac{2\pi}{7}$ and the step size is varied by letting $n = 2^k$ for $k = 0, ..., 9$.

From this experiment, we can see that the step size has a significant effect in prolonging the lifetime. In particular, it is neither good to move too much nor too little, but there is a step size that optimizes the lifetime. For comparison, we also show the performance of a static polar grid-based sink placement, which basically provides the baseline lifetime performance. Hence, this shows another time that sink mobility pays off, but most if the trajectory is designed carefully (in fact, random walk, outer periphery, and equal sectorization performed worse than the static polar grid). A zoom-in for the interesting range of n between 8 and 32, where the optimum step size lies for this experiment, is shown in Figure 11(b). As can be observed, the lifetime behavior is rather chaotic in this range, which hints at the difficulty of obtaining a closed form for the optimal step size under the polar grid, which we leave for future work.

VI. Conclusion and Outlook

In this paper, we addressed the problem of finding good trajectories for multiple mobile sinks in WSNs with respect to both, minimizing worst-case delay and maximizing the lifetime of the network. Due to its fundamental hardness, we resorted to a geometric interpretation of the problem for which we introduced and optimized a polar grid trajectory. The simulation results exhibited a very promising delay and lifetime performance for the polar grid trajectory when compared to other trajectories.

As the design space for possible sink trajectories is huge it is tempting to contemplate a bit about extensions as well alternatives to the polar grid trajectory. An obvious extension of the two orbits model used by our polar grid is to use n orbits. Going to n orbits, however, will be harder to optimize by enumeration as the search space for distributing K sinks over n orbits grows as $\binom{K-n-1}{n-1}$ (allowing orbits to be empty). Apart from applying heuristics for that search, one could strive for a closed-form expression over the maximal distances in the n-orbit polar grid to avoid this combinatorial explosion. While this seems hard it would constitute an important step in the general understanding of concentric trajectories.

Non-concentric, but still periodic (following a closed circuit) strategies are imaginable, for example a star shaped trajectory. As a generalization of the concentric class of strategies one may hope for further improvement under the assumption of a successful optimization. In fact, we have experimented with a specific (unoptimized) star-shaped trajectory, yet it was inferior to the polar grid trajectory.

Even for non-periodic trajectories, like the random walk, one may see a case if suitably enhanced. For example, a biased random walk which tries to avoid areas of low energy could perform well with respect to lifetime maximization, though this involves a certain state-dependence which may be undesirable in large-scale WSNs.

At last, we briefly want to discuss how to possibly relax certain assumptions we made throughout the paper leading to further future work items. Dispensing with the assumption of a circular field could certainly be interesting. One direct way may be to go for an ellipsoid shape, which would probably still allow for a similar approach to the one presented in this paper, based on a suitably generalized polar grid (probably with segments of unequal size within one orbit). Similarly, we have made assumptions on node homogeneity and uniform distribution of nodes. Both of these may be relaxed by going to a three-dimensional geometric interpretation of the original problem where the third dimension could capture, e.g., nodes with (initially) higher battery levels or areas of higher node density. Clearly, the problem will not become simpler, but based on the good experience we made with the geometric interpretation of the underlying problem, we believe that this could be a winning strategy also for such advanced problem settings.

References

[1] Crossbow technology inc. mpr-mib users manual, June 2007.

[2] S. Basagni, A. Carosi, E. Melachrinoudis, C. Petrioli, and Z. M. Wang. Controlled sink mobility for prolonging wireless sensor networks lifetime. *Wireless Sensor Network*, 14(6):831–858, December 2008.

[3] I. Chatzigiannakis, A. Kinalis, S. Nikoletseas, and J. Rolim. Fast and energy efficient sensor data collection by multiple mobile sinks. In *Proc. 5th ACM Int. Workshop. on Mobility Management and Wireless Access*, pages 25–32, 2007.

[4] S. Gao, H. Zhang, and S. Das. Efficient data collection in wireless sensor networks with path-constrained mobile sinks. In *Proc. IEEE WoWMoM*, October 2009.

[5] D. K. Goldenberg, J. Lin, A. S. Morse, B. E. Rosen, and Y. R. Yang. Towards mobility as a network control primitive. In *Proc. ACM MobiHoc*, pages 163–174, 2004.

[6] J. Luo. *Mobility in Wireless Networks: Friend or Foe - Network Design and Control in the Age of Mobile Computing*. PhD thesis, School of Computer and Communication Sciences, EPFL, Switzerland, 2006.

[7] I. Papadimitriou and L. Georgiadis. Maximum lifetime routing to mobile sink in wireless sensor networks. In *Proc. Int. Conf. on Software, Telecommunications and Computer Networks*, September 2005.

[8] W. Y. Poe, M. Beck, and J. B. Schmitt. Planning the Trajectories of Multiple Mobile Sinks in Large-Scale, Time-Sensitive WSNs. Tech. Report 381/11, University of Kaiserslautern, Germany, February 2011.

[9] J. B. Schmitt and U. Roedig. Sensor Network Calculus - A Framework for Worst Case Analysis. In *Proc. DCOSS*, June 2005.

[10] R. C. Shah, S. Roy, Sus. Jain, and W. Brunette. Data mules: Modeling a three-tier architecture for sparse sensor networks. In *Proc. IEEE SNPA*, pages 30–41, 2003.

[11] M. I. Shamos and D. Hoey. Closest-point problems. *Proc. 16th Annual Symposium on Foundations of Computer Science*, pages 151–162, 1975.

[12] R. Shokri, P. Papadimitratos, M. Poturalski, and J. P. Hubaux. A Low-Cost Method to Thwart Relay Attacks in Wireless Sensor Networks. Proj. Report IC-71, 2007.

[13] A. A. Somasundara, A. Kansal, D. D. Jea, D. Estrin, and M. B. Srivastava. Controllably mobile infrastructure for low energy embedded networks. *IEEE Transactions on Mobile Computing*, 5:958–973, 2006.

[14] R. Sugihara and R. K. Gupta. Optimizing energy-latency trade-off in sensor networks with controlled mobility. In *Proc. IEEE INFOCOM*, pages 2566–2570, April 2009.

[15] Z. M. Wang, S. Basagni, E. Melachrinoudis, and C. Petrioli. Exploiting sink mobility for maximizing sensor networks lifetime. In *Proc. 38th Hawaii Int. Conf. on System Sciences*, January 2005.